Hydrodynamic boundary conditions, correlation functions, and Kubo relations for confined fluids

Lydéric Bocquet and Jean-Louis Barrat
Laboratoire de Physique, Ecole Normale Supérieure de Lyon, 46 Allée d'Italie, 69007 Lyon, France
(Received 16 July 1993)

Dynamical correlation functions of a fluid slab confined between two solid walls are computed using a phenomenologial, hydrodynamic appoach that generalizes Onsager's principle of linear regression of fluctuations to inhomogeneous systems. The phenomenological results are compared to exact molecular-dynamics simulations on simple model systems. This comparison permits a determination of the phenomenological parameters that describe the hydrodynamics of the fluid slab and especially of the boundary conditions (BC's) that account for the presence of solid walls. In most cases, the hydrodynamic BC for the tangential velocity field is found to be a no-slip BC and must be applied in a plane that is separated from the solid by about one layer of fluid atoms. A set of formal relations between the parameters that characterize the hydrodynamic BC and the equilibrium correlation functions of the inhomogeneous fluid is also derived. These relations are analogous to the usual Green-Kubo equalities for the transport coefficients of bulk fluids.

PACS number(s): 68.15.+e, 05.40.+j, 47.27.Lx

I. INTRODUCTION

The static properties of thin liquid films have been a subject of constant interest in the past two decades and are presently rather well understood. Experimentally, the most spectacular results were obtained using surface force apparatus (SFA) which permit a direct measurement of the forces between two solid surfaces across a thin (from several nanometers down to a few angstroms) liquid film. Many of these developments are described in the book by Israelachvili [1]. At large length scales (i.e., much larger than a molecular diameter), the results are well described by continuum theories such as the Lifshitz theory of van der Waals forces. Such theories break down at molecular length scales, where the surface forces display a strong oscillatory behavior as a function of the distance between surfaces. Both numerical simulation [2] and density-functional theory [3] on simple models have been used to interpret such experimental results. The oscillations in the force are related to the layered structure induced in the fluid by the presence of solid walls, which usually extends over several molecular diameters into the fluid.

Dynamical properties of thin films have also been the subject of many recent investigations using SFA. Experiments involving either draining or shearing liquid films have been performed, with results that fall into two different classes. Very thin films (less than 7–8 molecular diameters) exhibit strongly enhanced apparent viscosities [4], or even an exotic "stick-slip" behavior, intermediate between that of an elastic solid and that of a viscous fluid [5]. The response of thicker films, on the other hand, can be described using the Navier-Stokes (NS) equations for a viscous newtonian fluid [6,7], supplemented by the usual "no-slip" boundary conditions (BC's) [8] at the solid surface. Such a description, however, requires that the (hydrodynamic) thickness of the film is treated as an adjustable parameter, which might perceptibly differ from the thickness measured using other (electrical, mechanical, or optical) methods. Such differences are often interpreted as indicating the existence of an "immobilized" layer of fluid that does not participate in the hydrodynamic flow. In most cases, the thickness of this layer is of the order of one molecular diameter [6,7]. This interpretation, however, does not have a microscopic foundation. The same is true for the no-slip boundary condition (i.e., the condition that the tangential fluid velocity vanishes), which is usually used to account for the presence of a solid boundary. This condition is usually taken as a postulate of macroscopic hydrodynamics, which can be justified *a posteriori* by checking the correctness of its consequences [8]. Microscopic considerations, on the other hand, do not in general lead to the no-slip boundary condition. In particular, the early kinetic theory calculations of Maxwell [9] predicted the existence of velocity slip at solid boundaries. Velocity slip is known to occur in rarefied gases [10] and could also be present in polymer melts [11]. Studying the dynamics of thin films, in which the boundary conditions can be expected to have a measurable effect, should therefore provide an interesting way of investigating the validity of the no-slip BC for ordinary newtonian fluids. The discrepancy mentioned above between different determinations of this film thickness is an indication that the usual description in terms of the NS equations and no-slip BC might not always be appropriate at small length scales. More precisely, a better understanding of the boundary conditions would be desirable in order to interpret such results. That the "hydrodynamic thickness" of a film can differ from other determinations of the thickness is not, in itself, a surprising result. Some arbitrariness is *a priori* present in the process of accounting for the presence of an interface at finite width by a boundary condition applied at an idealized, mathematical surface. This arbitrariness is devoid of consequences in macroscopic hydrodynamics. For thin films, however, the choice of different boundary condi-

tions can lead to very different interpretations of the experimental results. It is the purpose of this work to demonstrate that the arbitrariness in the choice of hydrodynamic boundary conditions at a liquid-solid interface can be avoided and that, under some reasonable assumptions, the appropriate BC can be determined from first-principles microscopic calculations.

In Sec. II we propose a phenomenological description of the dynamics of a fluid-solid interface. Our description combines a boundary condition that allows for velocity slip at the solid boundary with a generalization of Onsager's hypothesis of linear regression of fluctuations. Together with the phenomenological NS equations, the BC permits a complete description of hydrodynamic flows. Following the spirit of Onsager's hypothesis, we postulate that the dynamics of small fluctuations around an equilibrium state can be described by the macroscopic equations of motion, *including the boundary conditions.* This simple assumption allows us to explicitly compute a phenomenological form of the *equilibrium* time-dependent correlation function of the momentum density for a fluid slab confined between two solid boundaries. The result depends both on the transport coefficients of the fluid and on the parameters that characterize the boundary condition.

Section III is devoted to a verification of the correctness of our approach through extensive *equilibrium* molecular-dynamics (MD) simulations. These simulations provide an "exact" determination of the time-dependent correlation functions of a fluid slab. By comparing these exact results with the analytical expression obtained using the approach of Sec. II, we are able to validate this approach and to determine the relevant phenomenological parameters for model systems. Our philosophy here is different from that underlying much of the earlier simulation work on the dynamics of confined fluids [12–14]. We do not attempt to model a specific flow pattern using *nonequilibrium* MD, thereby avoiding all the problems (temperature control, high velocity gradients) inherent in nonequilibrium simulations. Rather, we take advantage of the richness present in the natural fluctuations of the system to simultaneously determine different phenomenological parameters. Our approach is therefore extremely close in spirit to the equilibrium methods commonly used to determine, through Green-Kubo formulas, the transport coefficient of bulk fluids [15], as opposed to more recent, nonequilibrium, techniques [16]. For the sake of completeness, and in order to check the consistency of both approaches, we also perform nonequilibrium simulations of selected systems. Finally, we mention that, although our approach is quite general, the simulations are performed on very simplistic systems. Our aim here is not to provide a realistic description of some particular liquid-solid interface, but rather to test general assumptions on the simplest possible models.

The fact that the phenomenological parameters characterizing a liquid-solid boundary can be obtained from an equilibrium simulation suggests that these parameters could be directly expressed in terms of equilibrium correlation functions. Indeed, in the case of bulk fluids, the use of Onsager's hypothesis allows one to obtain relationships between the phenomenological coefficients and the microscopic time-dependent correlation functions [17,18], which are known as Green-Kubo formulas. In Sec. IV we show that similar results can be obtained for the parameters characterizing the BC. The numerical evaluation of the BC parameters through these Green-Kubo like formulas, using MD simulation, yields results that are in agreement with those obtained in Sec. III using a more direct approach.

Our main conclusions are summarized in Sec. V. A preliminary account of this work has been published in Ref. [19].

II. PHENOMENOLOGICAL DESCRIPTION OF A CONFINED FLUID SLAB

A. Description of the liquid-solid interface

Due to the formidable difficulties inherent in a full treatment using, e.g., kinetic theory, very little analytical work has been done on the dynamics of a liquid flowing past a solid wall. The interesting results that have emerged from recent simulation work [13,20,12] have not been discussed in a statistical-mechanical framework. In fluid dynamics, it is usual to bypass the complexity of the microscopic problem by imposing a boundary condition on the hydrodynamic velocity field. The most commonly used BC is that of no slip: the tangential velocity of the fluid vanishes at a fixed solid boundary. Experimental evidence indicates that this BC is fully appropriate for the description of the flow of simple liquids at macroscopic scales. It has been shown [21], however, that for the "rough" walls that are used in such experiments, different "microscopic" BC would produce practically undistinguishable results. Therefore the success of the no-slip BC at macroscopic scales does not necessarily imply that it remains appropriate in experiments performed at nanometer scales. Moreover, we already mentioned that simple kinetic theory calculations do not in general result in a no-slip BC. The boundary condition that is considered in this paper is the simplest one that allows for a velocity slip at the liquid-solid boundary, namely,

$$\left.\frac{\partial v_\alpha(\mathbf{r},t)}{\partial z}\right|_{z=z_0} = \frac{1}{\delta} v_\alpha(\mathbf{r},t)|_{z=z_0} \quad (\alpha = x,y) \; . \tag{2.1}$$

Here the interface is parallel to the $z=0$ plane and $\mathbf{v}(\mathbf{r},t)$ is the velocity field. This BC interpolates linearly between the no-slip BC ($\delta=0$) and the perfect slip BC ($\delta=\infty$), which corresponds to a fluid near an ideally flat wall. The length δ is then the ratio of the fraction constant λ to the shear viscosity η of the fluid.

Equation (2.1) introduces two parameters δ and z_0. In the following, we refer to δ as the slipping length and to z_0 as the "hydrodynamic position" of the wall. z_0 locates the position at which the boundary condition on the macroscopic velocity field has to be applied. It is not obvious at first sight that δ and z_0 are two independent parameters. For instance, if the flow is a planar Couette flow (uniform velocity gradient), it is always possible to modi-

fy the boundary condition by shifting z_0 by some amount Δ and increasing δ by the same amount, without changing the flow pattern in the bulk of the fluid. In other words, for the planar Couette geometry, identical bulk flows would be induced by the motion of walls characterized by the set of parameters (z_0,δ) and $(z_0+\Delta,\delta+\Delta)$. If, as is the case in much earlier work [12,13], only this geometry is considered, the two parameters cannot be determined independently. One has therefore to resort to some arbitrary definition of z_0 in order, for example, to assess the presence of velocity slip at the boundary. If, however, more complex (e.g., Poiseuille) flows are considered, the two sets of parameters (z_0,δ) and $(z_0+\Delta,\delta+\Delta)$ no longer produce identical results for the bulk flow. Therefore it is in principle possible to distinguish between the BC associated with these two sets. The study of a single flow pattern, however, is not in general sufficient to provide a unique determination of all parameters, which means that the arbitrariness on the definition of slip is also present in the studies of Poiseuille flow [14]. In general, z_0 is taken to correspond to the position of the first layer of atoms in the solid, but this choice is indeed arbitrary. The method we employ in this paper provides a way of uniquely determining both z_0 and δ for a given solid-liquid boundary. This is done by using the fact that all types of flow patterns are naturally present in the *equilibrium fluctuations* of the system, so that all the necessary parameters can be directly obtained from the study of these fluctuations.

B. Regression of fluctuations in a confined fluid

In the following, we restrict our attention to a system made up of a fluid slab confined between two solid walls parallel to the xy plane. The distance between the two walls is denoted by L. As emphasized in Sec. I, some arbitrariness is always present in the definition of L, since the fluid-solid interface has a finite width. For large enough L, the dynamics of the fluid slab can be described by the usual *bulk* phenomenological NS equations (involving the bulk transport coefficients) supplemented by a BC at each solid wall. The BC is assumed to be of type (2.1) at each wall. The lower wall is characterized by the parameters z_0 and $\delta=\delta_0$ and the upper one by z_0+h and $\delta=\delta_h$. It should be clear from the discussion above that the distance h between the two hydrodynamic positions of the walls *a priori* differs from the arbitrarily defined wall to wall distance L. L is an input parameter that simply serves to describe the setup of the two walls with respect to each other. h, on the other hand, is a phenomenological parameter that serves to the description of the dynamics of the confined fluid. It is *a priori* unknown and can indeed depend on the nature of the fluid under consideration.

The NS equations describe the relaxation toward equilibrium of the confined fluid from an arbitrary initial state. For bulk fluids, the transport coefficients that appear in these equations are intimately related to the *hydrodynamic* (i.e., long-wavelength and low-frequency) limit of the time-dependent *equilibrium* correlation functions of the fluid [18]. The connection is achieved by assuming that the equilibrium fluctuations in the fluid obey the same phenomenological equations that characterize the relaxation from a nonequilibrium situation. This assumption was first introduced by Onsager [22] and is generally known as Onsager's principle of linear regression of fluctuations. In this work, we propose that this hypothesis can be generalized to the case of confined fluids, by assuming that the equilibrium fluctuations in a fluid slab obey both the NS equations and the phenomenological boundary conditions at the (hydrodynamic) walls. Under these assumptions, we can write the following equations for the evolution of a fluctuation in the momentum density $\mathbf{j}(\mathbf{r},t)$: if $\mathbf{r}$ belongs to the bulk (i.e., if $0<z<h$)

$$\partial_t \mathbf{j}(\mathbf{r},t)+\nabla P(\mathbf{r},t)-\frac{(\zeta+\eta/3)}{\rho_0}\nabla[\nabla_{\mathbf{r}}\cdot\mathbf{j}(\mathbf{r},t)] -\frac{\eta}{\rho_0}\nabla^2\mathbf{j}(\mathbf{r},t)=\mathbf{0} \quad (2.2)$$

and if $\mathbf{r}$ belongs to the hydrodynamic boundaries ($z=z_0$, and $z=z_0+h$)

$$\mathbf{j}_{\parallel}(\mathbf{r},t)=\delta_{\text{wall}}\frac{\partial}{\partial \mathbf{n}}\mathbf{j}_{\parallel}(\mathbf{r},t), \quad \mathbf{j}_{\perp}(\mathbf{r},t)=\mathbf{0}\ . \quad (2.3)$$

Here ρ_0 is the mass density inside the fluid slab, P is the pressure and η and ζ are the shear and bulk viscosities of the bulk fluid at the same temperature and density. The indices $\parallel$ and $\perp$ refer to the tangential and perpendicular components of the vector field considered. The vector $\mathbf{n}$ is normal to the wall.

Equations (2.2) and (2.3) *define* our phenomenological model for the confined fluid slab. We assume that this slab can be adequately modeled using the equations that are appropriate for an isotropic, unconfined bulk fluid, supplemented by BC. In particular, the transport coefficients appearing in (2.2) are assumed to be unaffected by the boundaries and the equations retain the symmetry properties of the usual NS equations. This description obviously is a reasonable one for large wall to wall distances, but it could break down at small separations. In this section, we investigate the consequences of our assumptions, postponing the evaluation of their correctness to Sec. III.

As in the case of bulk fluids, our equations can be greatly simplified by introducing the transverse momentum density

$$j_\alpha(z,t)=\frac{1}{L_x L_y}\int\int dx\,dy\, j_\alpha(\mathbf{r},t), \quad \alpha=x,y$$

where L_x and L_y are the lateral dimensions of the system, which is periodic in the x and y directions. It is easy show that this field obeys the diffusion equation

$$\left[\partial_t-\frac{\eta}{\rho_0}\partial_z^2\right]j_\alpha(z,t)=0\ , \quad (2.4)$$

with the two BC's

$$j_\alpha(z,t)|_{z=z_0}=\delta_0\partial_z j_\alpha(z,t)|_{z=z_0}\ , \quad (2.5a)$$

$$j_\alpha(z,t)|_{z=z_0+h} = -\delta_h \partial_z j_\alpha(z,t)|_{z=z_0+h} \ . \tag{2.5b}$$

The time-dependent correlation function of j_α is, as usual, defined by

$$C(z,z',t) = \langle j_\alpha(z,t) j_\alpha(z',0) \rangle \ , \tag{2.6}$$

where the angular brackets denote a thermodynamic average. For simplicity, we drop the component index α in the following. Our assumptions imply that this equilibrium correlation function obeys the following equations:

$$\left[\partial_t - \frac{\eta}{\rho_0} \partial_z^2 \right] C(z,z',t) = 0, \quad z_0 < z < z_0 + h \tag{2.7}$$

$$C(z,z',t)|_{z=z_0} = \delta_0 \partial_z C(z,z',t)|_{z=z_0} \ , \tag{2.8a}$$

$$C(z,z',t)|_{z=z_0+h} = -\delta_h \partial_z C(z,z',t)|_{z=z_0+h} \ . \tag{2.8b}$$

The general solution to these equations is given by

$$C(z,z',t) = \sum_{n=0}^{+\infty} \alpha_n(z') \Psi_n(z) \Gamma_n(t) \ , \tag{2.9}$$

where the Ψ_n are a set of orthonormal functions defined for $0 < z < h$ by

$$\Psi_n(z) = \psi_n \cos(\lambda_n z - \theta_n), \quad \Gamma_n(t) = e^{-\nu \lambda_n^2 t} \ , \tag{2.10}$$

the λ_n, θ_n, and ψ_n being solutions of

$$\begin{aligned} \tan(\lambda_n h) &= \frac{\lambda_n(\delta_0+\delta_h)}{\lambda_n^2 \delta_0 \delta_h - 1} \ , \\ \cos(\theta_n) &= \frac{\lambda_n \delta_0}{\sqrt{1+(\lambda_n \delta_0)^2}} \ , \\ \psi_n^2 &= \frac{h}{2} \left[1 + \frac{\sin(2\lambda_n h - 2\theta_n) + \sin(2\theta_n)}{2\lambda_n h} \right] . \end{aligned} \tag{2.11}$$

In (2.10), we have introduced the kinematic viscosity $\nu = \eta/\rho_0$. The function $\alpha_n(z')$ is determined by the knowledge of the initial condition

$$\alpha_n(z') = \int_0^h dz \, C(z,z',t=0) \Psi_n(z) \ . \tag{2.12}$$

Knowing the initial condition $C(z,z',t=0)$, we are thus able to explicitly compute $C(z,z',t)$. This initial condition can be obtained from equilibrium statistical mechanics, using the microscopic definition of the momentum density:

$$\mathbf{j}(\mathbf{r},t) = \sum_{i=1}^{N} \mathbf{p}_i(t) \delta(\mathbf{r} - \mathbf{r}_i(t)) \ , \tag{2.13}$$

where $\mathbf{r}_i$ and $\mathbf{p}_i$ are the position and momentum of particle i. In the canonical ensemble, $C(z,z',t=0)$ is simply given by

$$C(z,z',t=0) = k_B T \langle \hat{\rho}(z) \rangle \delta(z - z') \ , \tag{2.14}$$

where we have introduced a mass density $\hat{\rho}(z)$,

$$\hat{\rho}(z) = \sum_{i=1}^{N} m \delta(z - z_i(t)) \ . \tag{2.15}$$

For the purpose of comparison with constant energy MD simulations, we need to compute the static correlation function $C(z,z',t=0)$ in the *microcanonical* ensemble. We expect then a correction of order $1/N$ to Eq. (2.14). We have computed this correction using the method of Lebowitz, Percus, and Verlet [23]. The details of this calculation are described in Appendix A and its results can be summarized as follows.

(i) If the walls are ideally flat (i.e., if the interaction between the solid walls and the fluid atoms is invariant under translations parallel to the walls), the total momentum of the fluid in the direction parallel to the wall is a conserved quantity. The static correlation function is then

$$C(z,z',t=0) = k_B T \langle \hat{\rho}(z) \rangle \delta(z - z') - \frac{k_B T}{mN} \langle \hat{\rho}(z) \hat{\rho}(z') \rangle \ . \tag{2.16}$$

This correction is essential since it guarantees that the fluctuations in the momentum parallel to the walls vanish:

$$\left\langle \sum_{i=1}^{N} p_i^\alpha \sum_{j=1}^{N} p_j^\alpha \right\rangle = 0, \quad \alpha \in \{x,y\} \ . \tag{2.17}$$

(ii) If the walls are rough, then the total momentum parallel to the walls is no longer a conserved quantity. The $1/N$ correction to the canonical expression vanishes and the canonical result (2.14) is recovered. This shows that, whatever the roughness, it is sufficient to restore the thermal fluctuations of the total momentum:

$$\left\langle \sum_{i=1}^{N} p_i^\alpha \sum_{j=1}^{N} p_j^\alpha \right\rangle = Nmk_B T, \quad \alpha \in \{x,y\} \ . \tag{2.18}$$

In our phenomenological description of the fluid slab, the density is uniform and equal to ρ_0 for $0 < z < h$. The appropriate initial conditions for the phenomenological correlation functions are therefore

$$C(z,z',t=0) = k_B T \rho_0 \delta(z - z') - \frac{k_B T}{mN} \rho_0^2 \tag{2.19a}$$

for flat walls and

$$C(z,z',t=0) = k_B T \rho_0 \delta(z - z') \tag{2.19b}$$

for rough walls. When these initial conditions are inserted in Eqs. (2.12) and (2.9), a straightforward calculation yields

$$C(z,z',t) = \frac{2}{h} \rho_0 k_B T \sum_{n=0}^{+\infty} \Psi_n(z) \Psi_n(z') \exp(-\nu \lambda_n^2 t) \ , \tag{2.20}$$

for rough walls. For ideally flat walls (described phenomenologically by $\delta_0 = \delta_h = \infty$), the solution is still given by (2.20), with the term $n = 0$ excluded from the summation.

To close this section, we briefly consider two limiting cases of the BC(2.1), for which the correlation function can be obtained in a compact analytical form. For perfectly flat walls ($\delta_0 = \delta_h = \infty$) and for sticky walls

($\delta_0=\delta_h=0$), the Laplace transform $\tilde{C}(z,z',\omega)$ defined as

$$\tilde{C}(z,z',\omega)=\int_0^{+\infty} dt\, C(z,z',t)e^{-\omega t}, \quad \mathrm{Re}(\omega)\geq 0 , \tag{2.21}$$

can be summed explicitly using the equality

$$\sum_{n=1}^{+\infty}\frac{\cos(nx)}{n^2+\alpha^2}=\frac{\pi}{2\alpha}\frac{\cos\alpha(\pi-x)}{\sinh\alpha\pi}-\frac{1}{2\alpha^2}, \quad x\in[0,2\pi] . \tag{2.22}$$

Introducing the length $\lambda=(\nu/\omega)^{1/2}$, we obtain

$$\tilde{C}(z,z',\omega)=\rho_0 k_B T\frac{\lambda}{2\nu}\times\left\{\frac{\cosh\left[\frac{h-(z+z')}{\lambda}\right]+\cosh\left[\frac{h-|z-z'|}{\lambda}\right]}{\sinh\left[\frac{h}{\lambda}\right]}-\frac{2\lambda}{h}\right\} \tag{2.23}$$

for perfectly flat walls and

$$\tilde{C}(z,z',\omega)=\rho_0 k_B T\frac{\lambda}{2\nu}\left\{\frac{\cosh\left[\frac{h-|z-z'|}{\lambda}\right]-\cosh\left[\frac{h-(z+z')}{\lambda}\right]}{\sinh\left[\frac{h}{\lambda}\right]}\right\} \tag{2.24}$$

for sticky walls.

III. MD SIMULATIONS OF CONFINED FLUIDS

A. Strategy and model

In this section, we present a test of our phenomenological description for the time-dependent correlation functions against "exact" results for the same functions, obtained from MD simulations of a particular model. Our strategy is as follows. We first compute, using standard technique [15], the bulk viscosity η of a model fluid. We then compute time-dependent correlation functions of the momentum density for a slab of the same model fluid, now confined by solid walls. The results are fitted using the phenomenological expression (2.20), the adjustable parameters being h, δ_0, and δ_h. The best fit yields the desired phenomenological parameters characterizing the fluid-wall interface under study. Finally, we have checked the intrinsic character of these parameters, i.e., that each interface can be characterized by a set $(z_{\mathrm{wall}},\delta_{wall})$, which does not depend on the presence of the second interface. This was achieved by varying the wall to wall distance L and by using various combinations of upper and lower walls, with different microscopic characteristics. As a complementary test, we also perform several nonequilibrium simulations of planar Couette flows between solid walls for which the phenomenological parameters had been obtained in equilibrium simulations. This allows us to check the consistency of equilibrium and nonequilibrium approaches.

For practical reasons, the correlation function that was calculated in the course of the simulation was not $C(z,z',t)$, but rather its Fourier transform

$$\hat{C}(k,k',t)=\int dz\int dz' e^{ikz}e^{-ik'z'}C(z,z',t)=\langle\hat{j}_\alpha(k,t)\hat{j}_\alpha(-k',0)\rangle , \tag{3.1}$$

where $\hat{j}(k,t)$ is the Fourier component of the transverse momentum density,

$$\hat{j}_\alpha(k,t)=\sum_i e^{ikz_i}p_{\alpha,i} \quad (\alpha=x,y) . \tag{3.2}$$

We stress that the summation in (3.2) includes all the atoms in the fluid, irrespective of the value of their z coordinate. In the phenomenological approach, the confined fluid is modeled as a slab of thickness h. The momentum density in this slab (or equivalently its Fourier components) represents, however, the momentum density of the whole fluid, including those atoms whose z coordinate does not lie between $z=0$ and h. Of course, the mapping between the phenomenological model and the exact simulation results is, in principle, only valid in the limit of small wave vectors $k\ll 2\pi/\sigma$.

Finally, we define the diagonal part $F(k,t)$ of $\hat{C}(k,k',t)$ as

$$F(k,t)=\langle\hat{j}_\alpha(k,t)\hat{j}_\alpha(-k,0)\rangle . \tag{3.3}$$

For the sake of simplicity and efficiency, we restrict ourselves to the consideration of this diagonal part in the following. Because this diagonal part has a nonzero limit in the bulk limit, this diagonal part is much larger—and therefore less sensitive to statistical noise—than other, nondiagonal, components of the correlation function. It obviously contains less information than the original correlation function, since the system is not invariant by translation along the z direction. It is nevertheless

sufficient to obtain the BC parameters, as shown in the following sections.

The fluid we have chosen is a standard one component fluid of "soft spheres," i.e., atoms interacting through the purely repulsive pair potential $v(r)=\epsilon(\sigma/r)^{12}$. This fluid is confined between two solid walls perpendicular to the z axis. Periodic BC are imposed in the x and y directions. The walls are "inert," i.e., lack internal degrees of freedom. The interaction between the walls and the fluid atoms can be described by an external potential v_{wf} acting on the fluid, which we take of the form

$$v_{wf}(\mathbf{r})=\epsilon_{wf}\phi\left[\frac{\mathbf{z}-\mathbf{z}_l(\mathbf{x},\mathbf{y})}{\sigma}\right]+\epsilon_{wf}\phi\left[\frac{\mathbf{z}_u(\mathbf{x},\mathbf{y})+\mathbf{L}-\mathbf{z}}{\sigma}\right]. \tag{3.4}$$

Most of the calculations are done with a purely repulsive wall $\phi=1/z^{12}$ and $\epsilon_{wf}/\epsilon=1$ (Sec. III B–III D). In Sec. III E we present results for a strongly attractive wall, described by $\phi=1/z^9-1/z^3$ and $\epsilon_{wf}/\epsilon=15$. $z_u(x,y)$ and $z_l(x,y)$ respectively model the microscopic roughness of the upper and lower walls. Both z_u and z_l have a zero average value, so that the potential (3.4) describes two walls separated by a "physical" distance L. In all the simulations, the temperature is $T=1.0\epsilon/k_B$ and, far from the walls, the fluid has a uniform density $\rho_0=0.64m\sigma^{-3}$. A typical density profile $\langle\rho(z)\rangle$ of the confined fluid is shown in Fig. 1. In most runs, the system size is $N=500$ fluid atoms. Identical results are obtained with larger systems ($N=1372$ atoms). The simulations are carried out at constant energy, using the standard Verlet algorithm [15], with a time step $\tau=0.005(m\sigma^2/\epsilon)^{1/2}$. Typical runs extend over 10^5 time steps. The shear viscosity of the corresponding bulk thermodynamic state ($T=1.0\epsilon/k_B$ and $\rho_0=0.64m\sigma^{-3}$), obtained independently from an MD simulation of the bulk fluid, is $\eta=(0.60\pm0.05)(m\epsilon)^{1/2}\sigma^{-2}$.

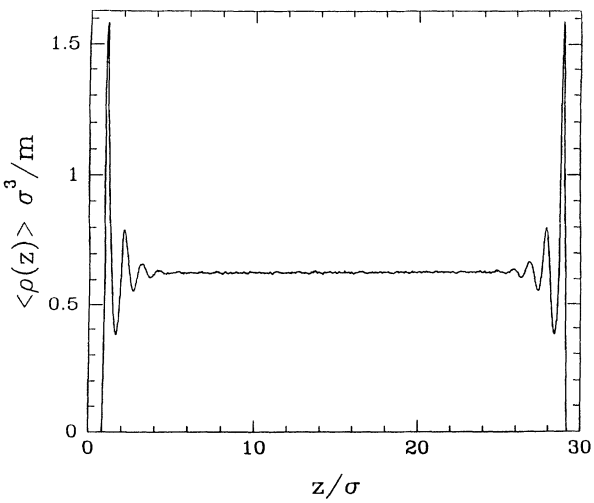

FIG. 1. Liquid density profile $\langle\rho(z)\rangle$ between two purely repulsive walls a distance $L=30\sigma$ apart. The average temperature was $T=1\epsilon/k_B$ and far from the walls the density was $\rho_0=0.64m\sigma^{-3}$.

B. Results for flat boundaries

We first study the case of purely repulsive and ideally flat walls $z_u(z,y)=z_l(x,y)=0$ separated by a distance $L=30.0\sigma$. There is no friction force at the boundaries, since no tangential momentum is exchanged between fluid and walls. Such walls should therefore be adequately described by pure slip BC $\delta_0=\delta_h=\infty$. The only parameter that can be adjusted to fit the experimental data is the hydrodynamical distance between walls h. We compare in Fig. 2 the phenomenological and simulated correlation function $F(k,t)$ for several values of k. The agreement is excellent provided the distance h is taken to be $h=(26.80\pm0.05)\sigma$. The initial time correlation function $F(k,0)$ obtained from (2.16) for the same value of h is compared in Fig. 3 to the simulation result. Again, the agreement is good and $F(k,0)$ clearly displays the behavior expected for a system in which the momentum parallel to the walls is a conserved quantity. We therefore conclude that the fluid slab can be adequately described by our phenomenological equations, the parameters describing the lower and upper interface being, respectively, ($z_0=1.6\sigma$ and $\delta_0=\infty$) and ($z_h=28.4\sigma$ and $\delta_0=\infty$). Inspection of the density profile $\langle\rho(z)\rangle$ shown in Fig. 1 shows that the hydrodynamic boundaries are located inside the fluid and are separated from the physical walls by one layer of fluid atoms.

C. Results for "corrugated" walls

In a next step, we introduce the possibility of tangential momentum transfer between the walls and the fluid by adopting for the solid walls a "corrugated iron" shape $z_u(x,y)=z_l(x,y)=u\cos(qx)$. The corrugation is characterized by its amplitude u and its wavelength $2\pi/q$. The

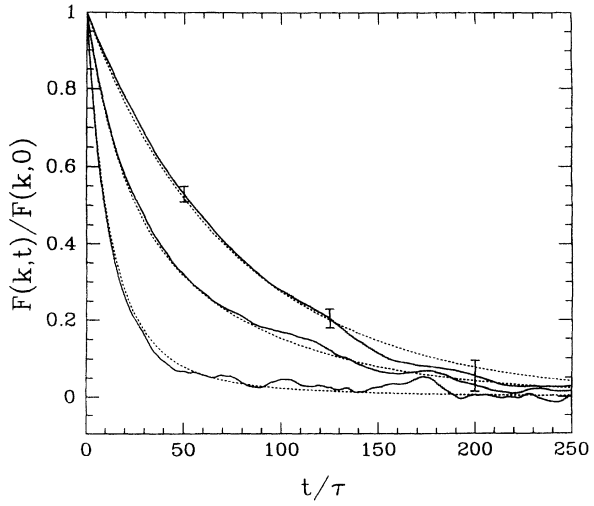

FIG. 2. Normalized correlation functions $F(k,t)/F(k,0)$ for a fluid confined between two perfectly flat walls. The curves correspond from top to bottom to $k\sigma=0.033$, 0.266, and 0.366. The solid lines are simulation results. The error bars, when present, are calculated on the basis of statistically independent runs. The dashed lines are calculated using Eq. (2.20) with $h=26.8\sigma$ and $\delta_0=\delta_h=\infty$.

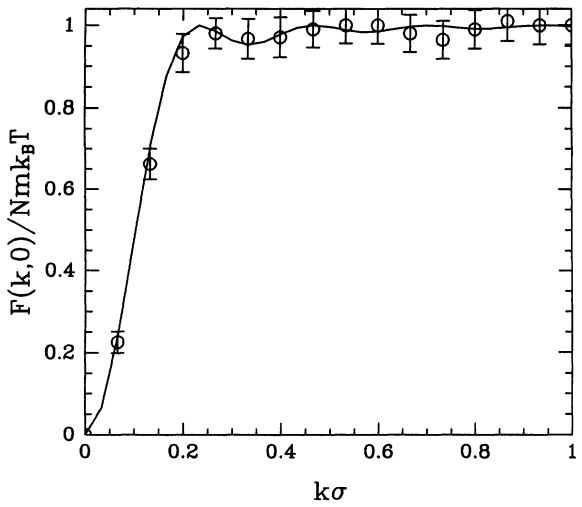

FIG. 3. Reduced initial time correlation function $F(k,0)/NmkBT$ as a function of $k\sigma$. The circles are simulation results. The dashed line is calculated using Eq. (2.19a) with $h=26.8\sigma$.

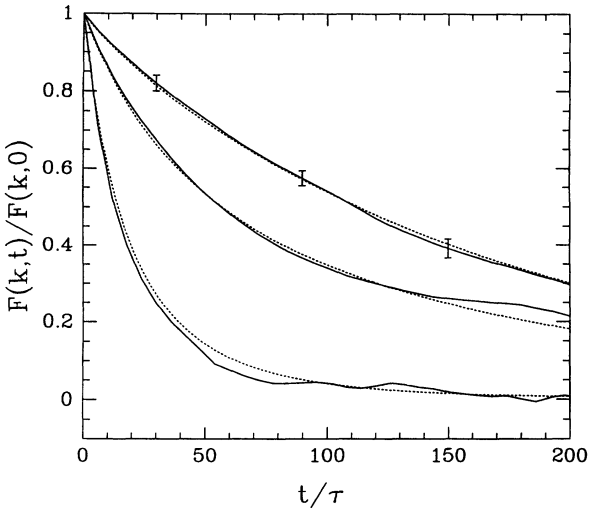

FIG. 4. Same as Fig. 1, but with two identical corrugated walls characterized by the parameters $u=0.02$, $2\pi q^{-1}=1$, and (from top to bottom) $k\sigma=0$, 0.166, and 0.3. The dashed lines represent the results of Eq. (2.20) with $h=26.8\sigma$ and $\delta_0=\delta_h=7.2\sigma$. Note that in this case the normalization is unnecessary since $F(k,0)=1$.

results, obtained for identical walls separated by $L=30.0\sigma$, can be summarized as follows. The equal time correlation function $F(k,0)$ is, as expected, given by (2.14). Correlations along the y direction are still described by the pure slip BC ($\delta_0=\delta_h=\infty$) and $h=26.8\sigma$. This simply reflects the fact that a wall moving in the y direction is unable to transfer momentum to the fluid. Correlations along the x direction, on the other hand, are in all cases very well fitted by Eq. (2.20), with $h=26.8\sigma$, and slipping lengths $\delta_0=\delta_h$ that depend on q and u. The results for the slipping lengths are summarized in Table I. Figure 4 shows a typical comparison between simulation data, obtained for $2\pi/q=1.0\sigma$ and $u=0.02\sigma$, and the best fit to the phenomenological results, which in that case is obtained for $h=26.8\sigma$ and $\delta_0=\delta_h=7.2\sigma$. The accuracy in the determination of the slipping length is about 0.05σ.

Two remarkable results emerge from these simulations. First, we find that the hydrodynamic separation between the walls is independent of the corrugation. This is probably related to the fact that, for the corrugations studied here, the density profiles in the direction perpendicular to the walls are practically undistinguishable from those obtained with perfectly flat walls. The hydrodynamic BC is in all cases separated from the physical walls by one layer of atoms. An inspection of the particle trajectories, however, did not reveal any indication of crystallization or locking in this layer. Both diffusion within the layer and exchange with the "bulk" part are apparent in the trajectories. Second, for corrugation amplitudes greater than 0.03σ, a no-slip BC is necessary to fit the simulation data. This corrugation is remarkably small, so that in practical cases one can expect the no-slip BC to hold even for molecularly smooth surfaces. On the other hand, the value 0.03σ is not to be taken too literally, since the wall potential (3.4) is corrugated over a longer range than the potential created by a wall made up of discrete atoms, in which the interference between the contribution of the different atoms causes the corrugation to fall off rapidly with the distance from the wall.

Earlier simulation work on the same subject [13,20,12] has been mostly concerned with the study of special flow patterns, namely planar Couette flow and Poiseuille flow. As explained in Sec. II A, these studies only give access to the combination $\delta+z_0$. Since these studies used a semirealistic modeling of the solid wall, no direct comparison

TABLE I. Phenomenological parameters describing various types of liquid-solid interfaces. The first and second columns give, respectively, the amplitude and wavelength of the corrugation. In all cases, the fluid-wall potential is purely repulsive. Columns 3 and 4 give the values of the parameters obtained by fitting the correlation functions (see Sec. III). Columns 5 and 6 give the results obtained by the Green-Kubo formulas (Sec. IV).

u/σ	$2\pi/q\sigma$	δ_{wall} (fit)	z_{wall} (fit)	δ_{wall} (GK)	z_{wall} (GK)
0		∞	1.60		
0.01	1	40.0±2.5	1.60±0.01	32	1.3
0.02	1	7.20±0.05	1.60±0.01	7.1	1.3
>0.03	1	0.00±0.02	1.60±0.01	0	1.3

with our results is possible. In most cases, i.e., for comparable solid and liquid densities, it was observed that one to two layers of fluid "stick" to the solid surface. This corresponds to $\delta+z_0\sim-\sigma$, in agreement with our conclusions. Much larger slipping effects were observed in the case where the solid has a much larger density than the liquid [12]. In an attempt to reproduce this effect, the wavelength of the corrugation was decreased to $2\pi/q=\sigma/2$ and $\sigma/4$, keeping the amplitude constant ($u=0.2\sigma$). A no slip BC was still found for these parameters. Here again, the amplitude of the corrugation is much stronger than the effective amplitude that results from summing up the interactions with discrete atoms, and this probably explains the absence of slip even in that case.

D. Intrinsic character of the BC parameters

We have shown in the two preceding sections that parameters appropriate for the description of a given fluid-solid interface can be obtained from the simulation of a fluid slab confined by two identical solid boundaries. It is of course desirable to check whether the parameters obtained are transferable, i.e., if they can be used to describe this same interface in a different geometry. To this aim, we study fluid slabs in which the upper and lower walls have different microscopic characteristics and for which the phenomenological parameters have been obtained in a previous study. The comparison between the phenomenological correlation function and the exact one is therefore free of adjustable parameters.

We first consider a system confined between a flat wall and a corrugated one (of characteristics $2\pi/q=1.0\sigma$ and $u=0.02\sigma$). Such a configuration should, according to the results presented above, be described by the phenomenological parameters $z_0=1.6\sigma$, $z_h=28.4\sigma$, $\delta_0=\infty$, and $\delta_h=7.2\sigma$. The correlation functions obtained with these phenomenological parameters are in excellent agreement with the simulation results, as shown in Fig. 5.

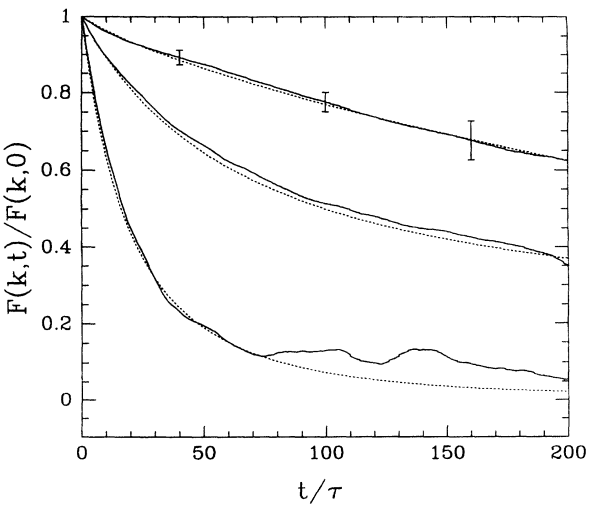

FIG. 5. Same as Fig. 4, but with the lower wall perfectly flat and the upper one characterized by the roughness parameters $u=0.02$ and $2\pi q^{-1}=1$. The dashed lines represent the results of Eq. (2.20) with $h=26.8\sigma$, $\delta_0=\infty$, and $\delta_h=7.2\sigma$. In this case, the phenomenological parameters of each wall-fluid interface have been obtained in previous studies, so that the comparisons are free of adjustable parameters.

Another way of checking the intrinsic character of phenomenological parameters is to study walls separated by various values of L. According to our model, the different configurations should be adequately represented by slipping lengths δ_0 and δ_h that do not depend on L and a distance between the hydrodynamic boundaries that differs from L by a constant term. We find that, for the values of L between 30σ and $L=12.0\sigma$, the phenomenological correlation function fits very well the simulated one without any adjustment of the parameters.

E. Attractive walls

In order to estimate the influence of an attraction (e.g., van der Waals attraction) between the fluid molecules and the solid walls, we use an attractive wall-fluid interaction described by a 9-3 Lennard-Jones form for ϕ, $\phi(z)=1/z^9-1/z^3$, and $\epsilon_{wf}/\epsilon=15$ [see Eq. (3.4)]. Both walls have identical corrugations, characterized by $2\pi/q=1.0\sigma$ and $u=0.2\sigma$. At short times, the hydrodynamic equations do not correctly describe the MD correlation functions. This discrepancy is likely due to the fact that, for such a strong attractive potential, epitaxial locking of the fluid particles in the grooves of the fluid-wall potential takes place. The dynamics of these locked particles is essentially solidlike and cannot be described using the equations of fluid dynamics. At longer times, the correlation functions in this simulation could still be fitted by the phenomenological form (2.20), with a slipping length equal to zero and $h\simeq 26.0$. The presence of a strong (only a large value of ϵ_{wf}, and therefore a deep potential well at the wall, was able to produce this effect) attractive part in the wall-fluid potential therefore causes the hydrodynamic thickness of the fluid slab to decrease. The hydrodynamic position of the BC is, in that particular case, separated from the physical wall by about two layers of fluid molecules.

F. Nonequilibrium simulations

A final test of our approach consists in performing nonequilibrium simulations for systems which have been fully characterized in equilibrium simulations. The flow pattern obtained in the nonequilibrium simulations can then be compared to the solution of the NS equations, with the BC's that have been obtained from the equilibrium simulations. Comparisons of this type, which do not involve any adjustable parameter, are shown in Fig. 6. The soft sphere fluid is confined between two identically corrugated walls. A planar Couette flow is imposed by moving the upper wall along x at a constant velocity $U=1.0(\epsilon/m)^{1/2}$. The flow pattern is entirely characterized by the average velocity profile $\langle v_x(z)\rangle$. The temperature is kept constant by introducing a frictional term (Hoover's thermostat [24]) in the equations of motion along the y direction. Two wall corrugations,

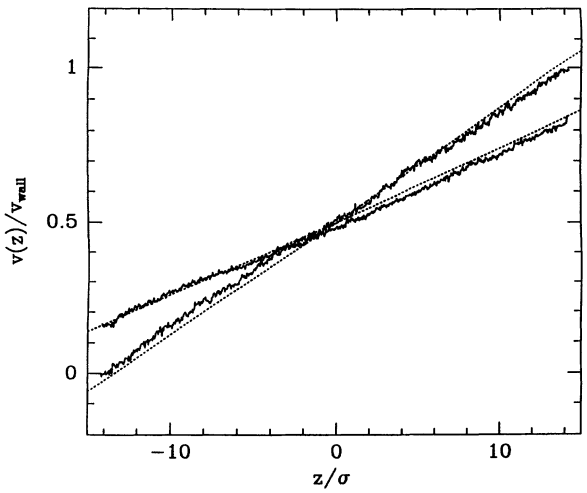

FIG. 6. Reduced velocity profile $v(z)/U$ inside the fluid slab in a Couette geometry. The velocity of the upper wall is $U=1.0(\epsilon/m)^{1/2}$. The solid lines are obtained from NEMD simulation for two wall corrugations, $2\pi/q=1.0\sigma, u=0.2\sigma$ (steep curve), and $2\pi/q=1.0\sigma, u=0.02\sigma$, and for a purely repulsive potential. The dashed lines are solutions of the NS equations and the slip BC [Eq. (2.1)], with, respectively, $\delta_{wall}=0\sigma$, $z_{wall}=1.6\sigma$ and $\delta_{wall}=7.2\sigma, z_{wall}=1.6\sigma$.

$2\pi/q=1.0\sigma, u=0.2\sigma$ and $2\pi/q=1.0\sigma u=0.02\sigma$, are considered. For the larger corrugation, both the purely repulsive potential of Sec. III C and the Lennard-Jones potential of Sec. III E are used. For the sake of clarity, only the two simulations with a purely repulsive potential are displayed in Fig. 6. The agreement between the simulated and calculated velocity profiles is seen to be excellent and confirms the validity of the equilibrium determination of the BC parameters.

IV. DISSIPATION COEFFICIENTS AND KUBO RELATIONS

The results obtained in Secs. III and IV lead to the following conclusions.

(i) The dynamics of the natural fluctuations in a confined fluid can be adequately described using phenomenological equations of motion and boundary conditions.

(ii) The simple BC (2.1) is sufficient to describe the properties of the fluid-wall interface.

For bulk fluids, it is well known that property (i) allows one to relate the phenomenological dissipation coefficients to the equilibrium time dependent correlation functions of the fluid. In this section, we derive similar relations for the phenomenological parameters z_{wall} and δ_{wall} appearing in (2.1).

A first relationship between the parameters that characterize a confined fluid slab can be obtained in the form of a "sum rule" involving the correlation function of the total momentum parallel to the walls $\hat{j}(k=0,t)=\sum_i p_{i,x}(t)$. The derivation of this sum rule is based upon applying linear-response theory to a fluid slab in which all molecules are subjected to a uniform force field F_0 in the x direction. An average current $\langle j_0 \rangle$ in the x direction will result from the application of this field. Linear-response theory yields

$$\langle j_0 \rangle = \left[\frac{\beta}{m} \int_0^{+\infty} dt \langle \hat{j}(0,t)\hat{j}(0,0) \rangle_{CE} \right] F_0 , \tag{4.1}$$

where $\beta=1/k_B T$ and $\langle\ \rangle_{CE}$ denotes a canonical ensemble average. An alternative expression for $\langle j_0 \rangle$ is obtained using the hydrodynamic description of the confined slab. In this picture, the force field generates a Poiseuille-like flow in the x direction with a velocity profile

$$v_x(z)=\frac{\rho_0 F_0}{2m\eta}\left[z^2 - z\frac{h^2+2\delta_h h}{h+\delta_0+\delta_h} - \delta_0 \frac{h^2+2\delta_h h}{h+\delta_0+\delta_h} \right] . \tag{4.2}$$

The resulting momentum flux in the x direction is

$$\langle j_0 \rangle = \int_0^h m v(z) dz = \frac{\rho_0 F_0}{12\eta}\left[1+3\frac{\delta_0+\delta_h+4\frac{\delta_0\delta_h}{h}}{H+\delta_0+\delta_h} \right] . \tag{4.3}$$

The identification of the two results (4.1) and (4.3) yields the sum rule

$$\int_0^{+\infty} dt \langle \hat{j}(0,t)\hat{j}(0,0) \rangle_{CE} = N\rho_0 k_B T \frac{h^2}{12\eta}\left[1+3\frac{\delta_0+\delta_h+4\frac{\delta_0\delta_h}{h}}{h+\delta_0+\delta_h} \right] . \tag{4.4}$$

The above derivation clearly illustrates the principles that underly the derivation of "Kubo-type" formulas for the BC parameters. The resulting sum rule, however, is not sufficient to independently determine all the phenomenological parameters. We have developed a more general approach to obtain explicit formulas for the parameters characterizing a planar fluid-solid interface. We present below a simple derivation of our results using linear-response theory. An alternative approach using the Mori-Zwanzig formalism is presented in Appendix B.

The system we consider is a fluid of viscosity η and density ρ_0, filling the upper half-space $z>0$ and bounded by a solid liquid interface in the $z=0$ plane. Here $z=0$ refers to the physical position of the interface, i.e., it has the same meaning as L in Sec. II. When a flow parallel to the wall is induced in the fluid, the net friction force acting on the fluid must be, according to the phenomenological description, proportional to the hydrodynamic velocity field computed at some position z_{wall} inside the fluid. The proportionality constant is of the form $S\lambda_{wall}$, where S is the interface area and λ_{wall} is the friction coefficient. The phenomenological parameters λ_{wall} and z_{wall} do not depend on the specific flow pattern or the external causes that generate this flow. This allows us to consider a particularly simple category of hydrodynamic flows, which can be generated by a simple perturbation of the system Hamiltonian. Our approach is inspired from the methods commonly used in nonequilibrium molecular dynamics (NEMD). In NEMD, homogeneous hydro-

dynamic flows or temperature gradients are created in a simulation cell by introducing fictitious force fields into Newton's equations of motion. Applying linear-response theory to these artificial fields, one recovers the usual Green-Kubo relations [16]. For example, the Green-Kubo relation for the shear viscosity can be obtained by applying linear-response theory to the perturbation Hamiltonian [24]

$$H[\nabla u]=\sum_{i=1}^{N}\mathbf{r}_i\mathbf{p}_i\cdot(\nabla\mathbf{u})^T . \tag{4.5}$$

This creates in the bulk fluid an hydrodynamic flow characterized by the strain rate tensor $(\nabla\mathbf{u})$ [the superscript T in (4.5) denotes a transposition]. To obtain the viscosity, one simply computes the stresses in the perturbed fluid to first order in (∇u) and one identifies the result to the usual Navier-Stokes form. We have extended this approach to the determination of the interfacial dissipation parameters, by considering perturbation Hamiltonians of the form

$$H[\dot\gamma,z_0]=\dot\gamma\sum_{i=1}^{N}(z_i-z_0)p_{i,x} . \tag{4.6}$$

This perturbation generates a Poiseuille flow in the x direction, characterized by the strain rate $\dot\gamma$. The velocity profile, computed to first order in $\dot\gamma$, is linear and vanishes for $z=z_0$,

$$v_x(z)=\dot\gamma(z-z_0) . \tag{4.7}$$

Linear-response theory gives the nonequilibrium average of any variable B in the presence of the perturbation as

$$\langle B\rangle_{\rm NE}(t)=-\frac{1}{k_BT}\int_0^t ds\,\langle B(t-s)\dot A(0)\rangle_{\rm CE}\dot\gamma(s) , \tag{4.8}$$

where the subscripts NE and CE denote, respectively, a nonequilibrium and a canonical average and $A=\sum_{i=1}^{N}(z_i-z_0)p_{i,x}$. The friction force $\langle F_x\rangle_{\rm NE}$ exerted by the wall on the fluid by the flow is obtained by specializing to $B=F_x$ in (4.8), which yields

$$\langle F_x\rangle_{\rm NE}(t)=\frac{\dot\gamma}{k_BT}\int_0^t ds\,\langle F_x(t-s)\dot A(0)\rangle_{\rm CE} . \tag{4.9}$$

The time derivative $\dot A$ can be expressed in terms of F_x and of the off-diagonal term of the stress tensor inside the fluid $\sigma_{xz}^{(f)}$,

$$\dot A=\sigma_{xz}^{(f)}-z_0F_x . \tag{4.10}$$

$\sigma_{xz}^{(f)}$ is defined as

$$\sigma_{xz}^{(f)}=\sum_{i=1}^{N}\left[\frac{p_{x,i}p_{z,i}}{m}+(F_{x,i}^{(f)}+F_{x,i}^{(w)})z_i\right] , \tag{4.11}$$

where $F_{x,i}^{(f)}$ and $F_{x,i}^{(w)}$ are the forces acting on particle i due, respectively, to the rest of the fluid and to the wall. If we now introduce $\lambda_{\rm wall}$ and $z_{\rm wall}$ defined as

$$\lambda_{\rm wall}=\frac{1}{Sk_BT}\int_0^{+\infty}ds\,\langle F_x(s)F_x(0)\rangle_{\rm CE}$$
$$z_{\rm wall}=\frac{\int_0^{+\infty}ds\,\langle F_x(s)\sigma_{xz}^{(f)}(0)\rangle_{\rm CE}}{\int_0^{+\infty}ds\,\langle F_x(s)F_x(0)\rangle_{\rm CE}} , \tag{4.12}$$

with $F_x=\sum_i F_{x,i}^{(w)}$ and S the interface area. Equation (4.9) can be cast into the final form [using (4.10) and (4.7)]

$$\langle F_x\rangle_{\rm NE}(t)=-S\lambda_{\rm wall}v(z_{\rm wall}) . \tag{4.13}$$

This expression is exactly similar to the phenomenological form for the friction force which reads

$$\langle F_x\rangle_{\rm NE}(t)=-S\frac{\eta}{\delta_{\rm wall}}v(z_{\rm wall}) . \tag{4.14}$$

Comparing the two expressions (4.13) and (4.14) provides the desired Green-Kubo expressions for the phenomenological parameters of the BC,

$$\delta_{\rm wall}=\frac{\eta}{\lambda_{\rm wall}} ,$$
$$\lambda_{\rm wall}=\frac{1}{Sk_BT}\int_0^{+\infty}ds\,\langle F_x(s)F_x(0)\rangle_{\rm CE} , \tag{4.15}$$

$$z_{\rm wall}=\frac{\int_0^{+\infty}ds\,\langle F_x(s)\sigma_{xz}^{(f)}(0)\rangle_{\rm CE}}{\int_0^{+\infty}ds\,\langle F_x(s)F_x(0)\rangle_{\rm CE}} . \tag{4.16}$$

It is easily checked that a shift in the origin of the z axis leaves $\delta_{\rm wall}$ invariant and shifts $z_{\rm wall}$ by the same amount. The parameters obtained using (4.15) and (4.16) are therefore intrinsic parameters, independent of the choice of the coordinate system. As noted before, (4.15) and (4.16) can also be obtained using the Mori-Zwanzig formalism, as shown in Appendix B.

The correlation functions appearing on the left-hand side of (4.15) and (4.16) could be computed in MD simulations. However, the evaluation of these formulas leads in finite systems to vanishing transport coefficients. This difficulty arises generally for any Green-Kubo coefficient Λ of the form $\Lambda\propto\int_0^\infty\langle\dot A\dot A(t)\rangle$, where is A is a dynamical variable (see [25] and references therein). To obtain a nonvanishing transport coefficient from this expression, the thermodynamic limit has to be taken before performing the integration to infinity, which is not possible in MD simulations. Several authors [26,27] have proposed a practical way to obtain an estimation of the previous integral by introducing a cutoff upper limit T_0 in the time integral. They proposed to choose T_0 as the first zero of the autocorrelation function. We have carried out an explicit evaluation of these formulas using this approximation for some of the systems studied in Sec. II. The results are reported in Table I. The agreement with the previous results is only fair and the approximate evaluation overestimates the friction [25] (and so underestimates the slipping length). The situation for the hydrodynamic position $z_{\rm wall}$ is even worse since it is expressed as a ratio of two integrals of correlation functions. However, a semiquantitative agreement is found, as seen in Table I.

V. SUMMARY AND CONCLUSIONS

In this paper, we have presented an alternative approach to the theory of hydrodynamic boundary conditions. Generally speaking, the description of the nonequilibrium behavior of a fluid under the action of external fields requires two ingredients: phenomenological transport coefficients and boundary conditions. It is well established that the transport coefficients are *intrinsic* properties of the bulk fluid. These coefficients can be measured independently of any boundary conditions by monitoring the relaxation of fluctuations in the bulk fluid, e.g., in inelastic light-scattering experiments. They can also, in principle, be computed from first principles using equilibrium statistical mechanics. Boundary conditions, on the other hand, are not, in general, derived from first-principle considerations. Rather, they usually appear as an additional hypothesis in the theory, whose consequences must be checked *a posteriori*.

Our work constitutes an attempt to avoid this difference in the treatment of transport coefficients and of boundary conditions. We have restricted our study to the boundary condition for the tangential velocity field in the fluid at a solid-liquid boundary, both because the problem is experimentally important and conceptually simple. Our approach consists in four steps. First, we specify the phenomenological form of the boundary condition, which will involve a few phenomenological parameters. Second, we compute the time-dependent correlation functions of the fluctuations in a confined fluid under the assumptions that the dynamics of these fluctuations obeys both the phenomenological equations of motion and boundary conditions. Third, we compare the computed correlation functions to exact results obtained from MD simulations. This allows us to confirm the validity of the phenomenological description and to obtain the corresponding parameters. Finally, we use the standard methods of statistical mechanics to explicitly relate the phenomenological coefficients of the BC to the equilibrium correlation functions of the fluid, computed in the presence of the boundaries. Evidently, these correlation functions now depend on the nature of both the fluid and the solid that form the interface. The approach is quite general and can be used for any type of solid-liquid interface, although in this paper we only considered the interface between an "inert" solid (i.e., a solid without internal degrees of freedom) and a liquid. It could also be generalized to the study of boundary conditions for other fields, e.g., temperature.

From a practical point of view, our most striking result is the fact that even extremely smooth solid surfaces are characterized by no-slip boundary conditions. For corrugations amplitudes larger than a few percent of the molecular diameter, velocity slip is absent at the solid boundary. This result is proven here only for the particularly simple system we considered, but we expect it to hold quite generally for simple fluids under standard conditions, since our system is quite typical of such fluids. Of course, the situation can be very different for polymers, in which another length scale, the chain size, must play an important role [11].

The second important result we derive is that the boundary condition on the hydrodynamic field must be applied at a surface that lies on the fluid side of the interface and is separated from the solid by about one layer of fluid atoms. This is true both of the no-slip BC which, as discussed above, holds in most cases and of the perfect slip BC that describes ideally flat walls. Again this result *a priori* is specific of the soft-sphere system we consider, but its validity probably is much more general. In fact, our result is qualitatively in perfect agreement with recent experimental observations [7] on a variety of simple molecular fluids. Also in qualitative agreement with these experimental observations is the fact that a strong attraction between the fluid molecules and the solid wall results in a decrease in the hydrodynamic thickness of the layer. Earlier simulation work [13,20,12] on Couette or Poiseuille flows also concluded, in most cases (see Sec. III C), to the existence of one or two "immobile" fluid layers at the solid liquid boundary. Our method permits a clearcut distinction between the position of the hydrodynamic BC and the slipping length itself, which cannot be found in earlier work.

Natural extensions of this work include the modelization of more realistic solid walls, the study of equilibrium correlations in strongly confined systems, and in systems presenting a fluid-fluid interface between two immiscible liquids. Such systems have been studied in the past using nonequilibrium methods [13,12,28–30], but we believe that the study of their equilibrium correlation functions could help understand their peculiar dynamical properties.

ACKNOWLEDGMENTS

Useful discussions or correspondence with J.-P. Hansen, M. O. Robbins, J.-M. Georges, and J.-L. Loubet are acknowledged. The Laboratoire de Physique is "Unité de Recherche Associée du CNRS No. 1325."

APPENDIX A

In this appendix, we obtain the relationship between the momentum fluctuations in the microcanonical and canonical ensembles [23]. We recall here only the main steps in the derivation, which is based on the method of Ref. [23].

We consider a system characterized by extensive variables $\{V_1, V_2, \ldots\}$, with conjugate intensive variables $\{X_1, X_2, \ldots\}$. For any quantity A, the average in the ensemble specified by variables $X_1, X_2, \ldots, \langle A | X_1, X_2, \ldots \rangle$ is related to the average computed in an ensemble specified by variables $V_1, V_2, \ldots, \langle A | V_1, V_2, \ldots \rangle$ through a Legendre transformation:

$$\langle A | X_1, X_2, \ldots \rangle = e^{\Psi(X_1, X_2, \ldots)} \int \cdots \int \langle A | V_1, V_2, \ldots \rangle \exp\left\{ -[\Psi(V_1, V_2, \ldots) + \sum_i X_i V_i] \right\} d\mathbf{V} , \tag{A1}$$

where the functions $\exp\{-[\Psi(X_1,X_2,\ldots)]\}$ and $\exp\{-[\Psi(V_1,V_2,\ldots)]\}$ are the partition functions of the system in each ensemble. In the thermodynamic limit, the exponent $\Psi(V_1,V_2,\ldots)+\sum_i X_i V_i$ in (A1) goes to infinity as $\langle N\rangle$ and the distribution in the $\{V_1,V_2,\ldots\}$ space becomes infinitely sharp. At finite $\langle N\rangle$, the average of A in the $\{\mathbf{X}\}$ ensemble is given by the average in the $\{\mathbf{V}\}$ ensemble plus corrections in powers of $\langle N\rangle^{-1}$. A Taylor expansion yields

$$\langle A|\langle\mathbf{V}\rangle\rangle=\langle A|\mathbf{X}\rangle+\tfrac{1}{2}\sum\frac{\partial}{\partial X_i}\frac{\partial X_i}{\partial V_i}\frac{\partial}{\partial\langle X_i\rangle}\langle A|\langle\mathbf{V}\rangle\rangle+\cdots . \tag{A2}$$

Applying (A2) to a product AB, the desired relation is obtained,

$$\begin{aligned}\langle\delta A\delta B|\mathbf{V}\rangle&=\langle AB|\mathbf{V}\rangle-\langle A|\mathbf{V}\rangle\langle B|\mathbf{V}\rangle\\&=\langle\delta A\delta B|\mathbf{X}\rangle\\&\quad+\sum\frac{\partial X_i}{\partial V_i}\frac{\partial\langle A|\mathbf{X}\rangle}{\partial X_i}\frac{\partial\langle B|\mathbf{X}\rangle}{\partial X_j},\end{aligned} \tag{A3}$$

where V_i means $\langle V_i|\mathbf{X}\rangle$.

We now specialize to the fluid slab studied in this work. We first consider the case where the walls are ideally flat. In the microcanonical ensemble, the x and y components of the total momentum $\mathbf{P}$ are conserved quantities and the extensive variables that characterize the system are the energy and the total momentum parallel to the walls (in addition to the volume V and the particle number N): (E,P_x,P_y). The conjugate intensive variables are, respectively, the inverse temperature β and the x and y components of the center of mass velocity v_x and v_y. Using (A3) we obtain the relation between the fluctuations in the microcanonical and canonical ensembles of any pair (A,B) of variables

$$\begin{aligned}\langle\delta A\delta B\rangle_{\mathrm{ME}}&=\langle\delta A\delta B\rangle_{\mathrm{CE}}-\frac{\beta^2}{NC/k_B}\frac{\partial\langle A\rangle_{\mathrm{CE}}}{\partial\beta}\frac{\partial\langle B\rangle_{\mathrm{CE}}}{\partial\beta}\\&\quad-\frac{\beta}{mN}\frac{\partial\langle A\rangle_{\mathrm{CE}}}{\partial\beta\mathbf{v}_\parallel}\frac{\partial\langle B\rangle_{\mathrm{CE}}}{\partial\beta\mathbf{v}_\parallel},\end{aligned} \tag{A4}$$

where the subscripts ME and CE, respectively, stand for microcanonical ensemble averages, C is the specific heat per particle, and $\mathbf{v}_\parallel$ is the vector (v_x,v_y). To derive (A4), we make use of the standard results:

$$\begin{aligned}\frac{\partial\langle E\rangle_{\mathrm{CE}}}{\partial\beta}&=-\langle(\delta E)^2\rangle_{\mathrm{CE}}=-N\beta^2C/k_B,\\\frac{\partial\langle P_i\rangle_{\mathrm{CE}}}{\partial\beta}&=-\langle\delta E\delta P_i\rangle_{\mathrm{CE}}=0,\\\frac{\partial\langle P_i\rangle_{\mathrm{CE}}}{\partial\beta v_j}&=\langle\delta P_i\delta P_j\rangle_{\mathrm{CE}}=Nm/\beta,\end{aligned} \tag{A5}$$

where $i,j\in\{x,y\}$. Applying (A4) with $A=\hat{j}(z,t)$ and $B=\hat{j}(z',t)$ [Eq. (2.13)], we obtain Eq. (2.16) of the main text.

For corrugated walls (i.e., the wall-fluid interaction depends on x and/or y), the total momentum parallel to the walls ceases to be a conserved quantity in the microcanonical ensemble and the system is characterized only by its energy (in addition to V and N). Using (A3) we now have

$$\langle\delta A\delta B\rangle_{\mathrm{ME}}=\langle\delta A\delta B\rangle_{\mathrm{CE}}-\frac{\beta^2}{NC/k_B}\frac{\partial\langle A\rangle_{\mathrm{CE}}}{\partial\beta}\frac{\partial\langle B\rangle_{\mathrm{CE}}}{\partial\beta}. \tag{A6}$$

The correction vanishes for the pair of variables $[\hat{j}(z,t),\hat{j}(z',t)]$, which yields Eq. (2.14).

APPENDIX B

In this appendix, we derive the Green-Kubo formulas for the phenomenological parameters δ_{wall} and z_{wall} within the Mori-Zwanzig formalism [18]. As in Sec. IV, we consider a single solid-fluid interface. The wall is located in the plane $z=0$ and the fluid fills the upper half-space $z>0$.

In the Mori-Zwanzig projection operator formalism, the (exact) evolution equations of any set of dynamical quantities $\mathbf{A}$ are written in the form of generalized Langevin equations,

$$\frac{d}{dt}\mathbf{A}(t)=i\boldsymbol{\Omega}\cdot\mathbf{A}(t)-\int_0^t d\tau\,\mathbf{M}(\tau)\cdot\mathbf{A}(t-\tau)+\mathbf{F}(t), \tag{B1}$$

where $\boldsymbol{\Omega}$ is the frequency matrix

$$\boldsymbol{\Omega}=\langle L\,\mathbf{A},\mathbf{A}^\dagger\rangle\cdot\langle\mathbf{A},\mathbf{A}^\dagger\rangle^{-1} \tag{B2}$$

and $\mathbf{M}(\tau)$ is the memory function matrix

$$\mathbf{M}(\tau)=\langle\mathbf{F}(\tau),\mathbf{F}^\dagger(0)\rangle\cdot\langle\mathbf{A},\mathbf{A}^\dagger\rangle^{-1}. \tag{B3}$$

$\mathbf{F}(\tau)$ is the random force, $\mathbf{F}(\tau)=\exp(i\mathcal{Q}L\tau)\mathbf{f}$, $\mathbf{f}=i\mathcal{Q}L\,\mathbf{A}$, and L is the Liouvillian. The operator $\mathcal{Q}$ is defined as $\mathcal{Q}=1-\mathcal{P}$, where $\mathcal{P}$ is the projector onto variables $\mathbf{A}$,

$$\mathcal{P}=\langle\ldots,\mathbf{A}^\dagger\rangle\cdot\langle\mathbf{A},\mathbf{A}^\dagger\rangle^{-1}\cdot\mathbf{A}. \tag{B4}$$

The angular brackets here stand for a *canonical* average. When the variables $\mathbf{A}$ relax much more slowly than all other properties, a time-scale separation (Markov approximation) is possible and leads to the following equations:

$$\frac{d}{dt}\mathbf{A}(t)=i\boldsymbol{\Omega}\cdot\mathbf{A}(t)-\boldsymbol{\Gamma}\cdot\mathbf{A}(t)+\mathbf{F}(t), \tag{B5}$$

where

$$\boldsymbol{\Gamma}=\int_0^{+\infty}d\tau\,\mathbf{M}(\tau) \tag{B6}$$

is the relaxation matrix. In addition, we will assume as usual that in the hydrodynamic limit (i.e., the zero wave vector limit) the time evolution of the memory functions is governed by the propagator $\exp(iL\tau)$. The memory functions are then equal to the corresponding time correlation functions.

Let us consider now the set of variables $\mathbf{A}=\{j_k\}$, when $j_k=\sum_i p_{x,i}\exp(ikz_i)$ is a Fourier component of the transverse fluid momentum density parallel to the wall. Because of the presence of the wall, these variables are not conserved and their correlation time does not go to

infinity when the wave number goes to zero, as opposed to the bulk case. However, we expect the lifetime of these variables to be still *macroscopic* compared with *microscopic* relaxation times, so that the Markov approximation is valid. In terms of these variables, (B5) can be rewritten

$$\frac{d}{dt}j_k(t)=\int dk'[i\Omega](k,k')\cdot j_{k'} - \int dk'[\Gamma](k,k')\cdot j_{k'}+F_k(t) \ . \tag{B7}$$

A straightforward calculation shows that $[i\Omega](k,k')$ is equal to zero. The relaxation matrix can be written

$$\Gamma(k,k')=\int_0^{+\infty}d\tau[\langle \mathbf{F}(\tau),\mathbf{F}^\dagger(0)\rangle\cdot\langle \mathbf{A},\mathbf{A}^\dagger\rangle^{-1}](k,k') = \int dk''[\tilde{\Gamma}](k,k'')[\langle \mathbf{A},\mathbf{A}^\dagger\rangle^{-1}](k'',k') \ , \tag{B8}$$

where we introduced $\tilde{\Gamma}$ defined as

$$\tilde{\Gamma}=\int_0^{+\infty}d\tau\langle \mathbf{F}(\tau),\mathbf{F}^\dagger(0)\rangle \ . \tag{B9}$$

The matrix $\langle \mathbf{A},\mathbf{A}^\dagger\rangle^{-1}$ can be written in the alternative form, using the equilibrium mass density profile $\rho(z)$,

$$[\langle \mathbf{A},\mathbf{A}^\dagger\rangle^{-1}](k,k')=\int dz\frac{e^{i(k-k')z}}{(2\pi)^2k_BT\rho(z)} \ . \tag{B10}$$

Using (B8) and (B10), we then compute the second term in the right-hand side of (B7),

$$\int dk'[\Gamma](k,k')\cdot j_{k'}=\frac{1}{(2\pi)^2k_BT}\int dk''[\tilde{\Gamma}](k,k'')\int dz\, e^{ik''z}\frac{1}{\rho(z)}\int dk' j_{k'}e^{-ik'z}=\frac{1}{2\pi k_BT}\int dk''[\tilde{\Gamma}](k,k'')v_{k''} \ . \tag{B11}$$

In Eq. (B11), we have introduced the hydrodynamic velocity field $v(z)$ (and its Fourier transform v_k) defined as $v(z)=j(z)/\rho(z)$, where $j(z)$ is the momentum density, related to its Fourier components through

$$\int dk' j_{k'}e^{-ik'z}=2\pi j(z) \ . \tag{B12}$$

The time evolution of j_k is thus given by

$$\frac{d}{dt}j_k(t)=-\frac{1}{2\pi k_BT}\int dk'[\tilde{\Gamma}](k,k')v_{k'}+F_k(t) \ , \tag{B13}$$

which shows that the x component of the force acting on the fluid due to the wall F_x^{wall} is related to the hydrodynamic velocity field through

$$F_x^{\text{wall}}(t)=\frac{d}{dt}P_x(t)=\frac{d}{dt}j_{k=0}(t)=-\frac{1}{2\pi k_BT}\int dk'[\tilde{\Gamma}](k=0,k')v_{k'}+F_{k=0}(t) \ , \tag{B14}$$

where $P_x=\sum_i p_{x,i}$ is the total momentum parallel to the wall.

In the limit of small k, the matrix $\tilde{\Gamma}$ is simply

$$\tilde{\Gamma}=\int_0^{+\infty}d\tau\langle F_x(\tau)F_x(0)\rangle+i(k-k')\int_0^{+\infty}d\tau\langle F_x(\tau)\sigma_{xz}(0)\rangle+O(k^2,\ldots) =\lambda_{\text{wall}}Sk_BT[1+i(k-k')z_{\text{wall}}+O(k^2,\ldots)] \ , \tag{B15}$$

where $F_x(t)$ is the instantaneous force acting on the fluid due to the wall, $\sigma_{xz}(t)$ is stress tensor inside the fluid, S is the interface area, and the two parameters λ_{wall} and z_{wall} are defined by Eq. (4.12). In the phenomenological approach, the force acting on the fluid depends only in the hydrodynamic velocity field. Therefore only small k' are involved in the integration in (B14) and we can write

$$F_x^{\text{wall}}(t)=-\lambda_{\text{wall}}S\frac{1}{2\pi}\int dk'[1-ik'z_{\text{wall}}+O(k'^2)]v_{k'}+F_{k=0}(t) \simeq -\lambda_{\text{wall}}Sv(z=z_{\text{wall}})+F_{k=0}(t) \ . \tag{B16}$$

In the Markov approximation, the random term $F_{k=0}(t)$ can be neglected after a transient time much shorter than the hydrodynamic time scale, which yields the final result

$$F_x^{\text{wall}}(t)=-\lambda_{\text{wall}}Sv(z=z_{\text{wall}}) \ . \tag{B17}$$

[1] J. N. Israelachvili, *Intermolecular and Surface Forces* (Academic, London, 1985).
[2] L. K. Snook and W. van Megen, J. Chem. Phys. **72**, 2907 (1980).
[3] R. Evans, in *Liquids at Interfaces*, J. Charvolin, edited by J. F. Joanny and J. Zinn-Justin (North-Holland, Amsterdam, 1990).
[4] H. W. Hu, G. A. Carson, and S. Granick, Phys. Rev. Lett. **66**, 2758 (1991).
[5] J. N. Israelachvili, P. M. McGuiggan, and A. M. Homola,

Science **240**, 189 (1988).
[6] D. Y. C. Chan and R. G. Horn, J. Chem. Phys. **83**, 5311 (1985).
[7] J.-M. Georges, S. Millot, J.-L. Loubet, and A. Tonck, J. Chem. Phys. **98**, 7345 (1993).
[8] G. K. Batchelor, *An Introduction to Fluid Dynamics* (Cambridge University Press, Cambridge, 1967).
[9] J. C. Maxwell, Philos. Trans. R. Soc. London Ser. A **170**, 213 (1979).
[10] M. K. Kogan, *Rarefied Gas Dynamics* (Plenum, New York, 1959).
[11] P. G. de Gennes, C. R. Acad. Sci. Paris B **288**, 219 (1979).
[12] P. A. Thompson and M. O. Robbins, Phys. Rev. A **41**, 6830 (1990).
[13] J. Koplik, J. R. Nanavar, and J. F. Willemsen, Phys. Rev. Lett. **60**, 1282 (1988).
[14] M. Sun and C. Ebner, Phys. Rev. Lett. **69**, 1491 (1992).
[15] M. Allen and D. Tildesley, *Computer Simulation of Liquids* (Oxford University Press, Oxford, 1987).
[16] D. J. Evans, in *Molecular-Dynamics Simulation of Statistical-Mechanical Systems,* edited by G. Ciccotti and W. G. Hoover (North-Holland, Amsterdam, 1986).
[17] E. Helfand, Phys. Rev. **119**, 1 (1960).
[18] D. Forster, *Hydrodynamic Fluctuations, Broken Symmetry and Correlation Functions* (Benjamin Cummings, Reading, MA 1975).
[19] L. Bocquet and J.-L. Barrat, Phys. Rev. Lett. **70**, 2726 (1993).
[20] U. Heinbuch and J. Fischer, Phys. Rev. A **40**, 1144 (1989).
[21] S. Richardson, J. Fluid Mech. **59**, 707 (1975).
[22] L. Onsager, Phys. Rev. **37**, 405 (1931); **38**, 2265 (1931).
[23] J. L. Lebowitz, J. K. Percus, and L. Verlet, Phys. Rev. **153**, 250 (1967).
[24] W. G. Hoover, *Computational Statistical Mechanics* (Elsevier, Amsterdam, 1991).
[25] P. Español and I. Zúñiga, J. Chem. Phys. **98**, 574 (1993).
[26] A. N. Largar'kov and V. H. Sergeev, Usp. Fiz. Nauk **125**, 409 (1978) [Sov. Phys. Usp. **27**, 566 (1978)].
[27] J. J. Brey and J. Gomez Ordonez, J. Chem. Phys. **76**, 3260 (1982).
[28] P. A. Thompson and M. O. Robbins, Phys. Rev. Lett. **63**, 766 (1989).
[29] S. A. Somers and H. T. Davis, J. Chem. Phys. **96**, 5389 (1992).
[30] P. A. Thompson, G. S. Grest, and M. O. Robbins, Phys. Rev. Lett. **68**, 3448 (1992).